AN EVALUATION OF HYBRID VERSUS STOCHASTIC GROUND MOTION SIMULATIONS IN TERMS OF EARTHQUAKE ENGINEERING PARAMETERS

E. Ozmen[1], S. Karimzadeh[2] and A. Askan[3]

[1]*Graduate Student, Civil Eng. Department, METU, Ankara, Turkey*
[2]*Inst. Dr., Civil Eng. Department, METU, Ankara, Turkey*
[3]*Prof. Dr., Civil Eng. Department, METU, Ankara, Turkey*
Email: ekin.ozlu@metu.edu.tr

ABSTRACT:

Full ground motion time histories are essential inputs for several engineering applications. It is important to use realistic ground motions for accurate engineering analyses. Whenever observed records are insufficient or unavailable, simulations constitute reliable alternatives. Use of simulations based on regional seismotectonic and geological information have been initiated within the last decade globally. Due to the strong tradeoff between the cost and accuracy of the simulation methods, assessment of these simulated motions is still a topic of research. In this study, Duzce located in Western Turkey is selected as the study area. In the selected region, two common approaches for ground motion simulation are evaluated in terms of different earthquake engineering parameters. These methods are the stochastic finite-fault and hybrid ground motion simulation approaches. The first method is more practical while the second one is more accurate but requires detailed input data. Comparisons are performed for different past and scenario earthquakes in terms of PGA, PGV, spectral amplitudes at different period ranges for past and potential scenario events. Finally, the results are compared with respect to the existing global and local ground motion prediction equations.

KEYWORDS: Ground motions, stochastic finite-fault simulation, hybrid simulation, potential large earthquakes, earthquake engineering parameters

1. INTRODUCTION

The devastating effects of earthquakes are obvious in urban regions with high population. The extent of damage and losses can be evaluated by ground motion simulations in areas with high seismic activity and insufficient seismic network.

In literature, three types of ground motion simulations are performed: Deterministic, stochastic and hybrid simulations. Ground motion simulations involve mathematics, numerical analysis, and geophysics theory. As input, seismological properties in terms of source path and site parameters are required. Deterministic method simulates low frequencies, stochastic method models the high frequencies and hybrid method simulates the whole frequency range. (e.g.: Kamae et al. 1998; Hartzell and Harmsen 1999; Motazedian and Atkinson, 2005; Frankel 2009; Mai et al. 2010).

The objective of this study is to compare two alternative ground motion simulation methods used for the simulation of the 1999 Duzce (M_w=7.1) earthquake and two scenario events (M_w=6.5 & 6.0): Stochastic and broadband ground motion simulations. The results of the stochastic and broadband ground motion simulations are initially compared against the recorded data followed by a comparison with one local and one global Ground Motion Prediction Equations (GMPE's) in terms of peak ground acceleration (PGA) and peak ground velocity (PGV). It

is observed that the broadband simulation provides better results compared to the only stochastic one performed by Karimzadeh et al. (2017).

2. STUDY REGION

The study region is Duzce which is located on the North Anatolian Fault Zone (NAFZ) in Turkey with a right-lateral strike-slip faulting mechanism. This area is studied herein due to its high seismicity where two major earthquakes occurred within a short time span in 1999: The first one is the 17 August 1999 Kocaeli earthquake with Mw=7.4, whereas the second one, also of interest in this study, is the 12 November 1999 Duzce event (Mw=7.1). Duzce city is built on an alluvial basin, which cause basin effects during earthquakes in addition to amplifications due to soft soil conditions (Asten et al., 2014). In Figure 1, the major earthquakes which occurred on NAFZ during the last century are shown while the red box shows the Duzce region.

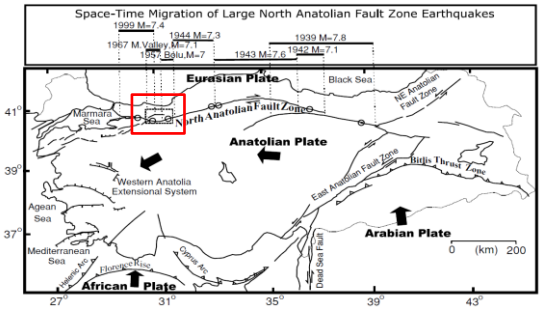

Figure 1. Tectonic Map of Turkey and major earthquakes on the NAFZ (adapted from Utkucu et. al., 2003)

3. METHODOLOGY

The methodology for ground motion simulation is explained briefly: The broadband ground motion simulation method used herein combines the low and high frequency motions in the frequency domain. The low frequency range is simulated based on the discrete wavenumber finite element method (DWFE) (deterministic method) (Olson et al., 1984) and the high frequency portion is simulated using the stochastic finite fault method Motazedian and Atkinson, 2005)

3.1. Deterministic Strong Ground Motion Simulation Methodology

Deterministic strong ground motion simulations are performed with the DWFE method (Olson et al., 1984) to simulate the low frequency portion of ground motions. DWFE method employs finite element method to solve the elastic equations for horizontal seismic wavefield while it uses finite differences to obtain numerical solutions for vertical wavefield and time dependence. COMPSYN program as implemented by Spudich and Archuleta (1987) is used in this study to obtain ground motions within the low frequency range.

The main inputs are the hypocenter, fault mechanism, seismic moment, and slip model on the fault plane, and parameters for the velocity model which are the layer thicknesses, the corresponding P and S wave velocities and density.

3.2. Stochastic Strong Ground Motion Simulation Methodology

Stochastic strong ground motion simulations are implemented for high frequency range using the finite-fault method based on a dynamic corner frequency approach. For this purpose, EXSIM program (Motazedian and Atkinson, 2005) is used herein. In this methodology, fault plane is divided into small rectangular subfaults, where each subfault is modeled as a point source which contributes to the total acceleration with kinematic delays.

In the stochastic finite fault model, it is assumed that the rupture starts to spread radially from the hypocenter. The ground acceleration is obtained as the summation of all subfault accelerations with kinematic time delays. The final acceleration spectrum is obtained in terms of source, path, and site effects as:

$$A_{ij}(f) = CM_{0ij}H_{ij}\frac{(2\pi f)^2}{\left[1+\left(\frac{f}{f_{c_{ij}}}\right)^2\right]}e^{-\frac{\pi f R_{ij}}{Q(f)\beta}}G(R_{ij})A(f)e^{-\pi\kappa f} \quad (1)$$

where $C = \frac{\Re^{\theta\varphi}\cdot\sqrt{2}}{4\pi\rho\beta^3}$ is a scaling factor, $\Re^{\theta\varphi}$ is the radiation pattern, ρ is the density, β is the shear-wave velocity, $M_{0_{ij}} = \frac{M_0 S_{ij}}{\sum_{k=1}^{nl}\sum_{l=1}^{nw} S_{kl}}$ is the seismic moment, S_{ij} is the relative slip weight and $f_{c_{ij}}(t)$ is the dynamic corner frequency of ij^{th} subfault where $f_{c_{ij}}(t) = N_R(t)^{-1/3}4.9\times10^6\beta\left(\frac{\Delta\sigma}{M_{0_{ave}}}\right)^{1/3}$. Here $\Delta\sigma$ is the stress drop, $N_R(t)$ is the cumulative number of ruptured subfaults at time *t*, and $M_{0_{ave}} = M_0/N$ is the average seismic moment of subfaults. R_{ij} is the distance from the observation point, $Q(f)$ is the quality factor, $G(R_{ij})$ is the geometric spreading factor, $A(f)$ is the site amplification term, and $e^{-\pi\kappa f}$ is a high-cut filter to include the spectral decay at high frequencies described with the κ factor of soils. H_{ij} is a scaling factor introduced to conserve the high-frequency spectral level of the subfaults.

3.3. Broadband (Hybrid) Ground Motion Simulation Approach

Broadband ground motions are obtained by a combination of the deterministic and stochastic methods as mentioned above. The combination is performed following the hybridization approach of Mai and Beroza (2003). For this purpose, COMPEX program as implemented in Moratto et al. (2015) is employed herein.

The Fourier amplitude spectra of the low and high frequency seismograms are combined in the frequency domain as:

$$A(f) = A^{LF}(f)\cdot W^{LF}(f) + A^{HF}(f)\cdot W^{HF}(f) \quad (2)$$

where *A(f)* is the broadband spectrum, $A^{LF}(f)$ is the low frequency spectrum and $A^{HF}(f)$ is the high frequency spectrum. $W^{LF}(f)$ and $W^{HF}(f)$ are the smoothed frequency-dependent weighing functions for the low and high frequencies, respectively.

In COMPEX, a crossover frequency (f_{match}) is selected to merge the low and high frequency portions. To obtain broadband ground motions in the time domain in COMPEX, inverse Fourier transform is applied to the broadband amplitude and phase spectra.

4. RESULTS

The stochastic and broadband ground motion simulations for the 1999 Duzce earthquake and for scenario earthquakes with M_w=6.5 and M_w=6.0 are performed at 4 selected stations (BOL, DZC, GYN and SKR) located within an epicentral distance less than 100 km. The input parameters for the stochastic ground motion simulation of the 1999 Duzce earthquake are previously validated by Ugurhan and Askan (2010) and then modified by Karimzadeh et al. (2017) whereas the input parameters for the broadband ground motion simulation of this event are obtained by Ozmen et al. (2019). Thus, the simulation parameters corresponding to both techniques for the 1999 Duzce earthquake and the scenario events are taken from the mentioned previous studies. At the selected 4 stations, comparison of the results in terms of PGA and PGV corresponding to the only-stochastic and broadband ground motion simulations versus the real values are given in Table 1.

Table 1 Comparison of the real, only-stochastic, and broadband results in terms of the PGA and PGV values at the selected four stations

Stations	Directions	PGA (cm/s²)					PGV (cm/s)				
		Real	Broadband Simulation	Stochastic Simulation	GMPE 1 - BA08	GMPE 2 - AC10	Real	Broadband Simulation	Stochastic Simulation	GMPE 1 - BA08	GMPE 2 - AC10
BOL	(E-W)	805.88	741.36	313.25	255.15	197.39	66.61	60.99	13.72	26.91	20.30
	(N-S)	739.51	584.37				57.78	74.19			
DZC	(E-W)	513.78	-	332.32	521.91	367.97	90.78	-	70.69	65.34	36.69
	(N-S)	407.69	-				66.47	-			
GYN	(E-W)	25.82	41.10	55.50	131.73	62.68	8.68	2.82	4.53	12.18	8.77
	(N-S)	27.89	55.76				9.84	5.26			
SKR	(E-W)	24.72	57.17	91.87	158.68	83.54	5.17	4.27	15.48	14.78	10.75
	(N-S)	17.33	48.89				4.81	2.76			

The results of both broadband and only-stochastic simulations are also compared against the selected two recent ground motion prediction equations (GMPE): Boore and Atkinson in (2008 BA08) and Akkar and Cagnan in (2010 AC10). The comparisons are made in terms of the PGA and PGV values at the four stations (BOL, DZC, GYN & SKR) which recorded the 1999 Duzce earthquake (Mw=7.1), and for the scenario earthquakes of M_w=6.5 and M_w=6.0 (Figures 2-7). As shown in Figures 2-5, PGA values of the broadband results give better match with AC10, compared to stochastic results. Results of only-stochastic ground motion simulations at some nodes are overestimated for PGA and PGV values for scenario earthquakes of M_w=6.0 and M_w=6.5 (Figures 2-5). These discrepancies may be occurred due to the lack of accuracy in the simulation of the low frequencies. In Figures 6 and 7, comparisons of the PGA and PGV values for both broadband and stochastic results with GMPE's are given. As shown in Figure 6, the broadband results give closer match with both BA08 and AC10 compared to the stochastic results.

Next, the spatial distributions of the simulated PGA and PGV values are obtained for the 1999 Duzce (M_w=7.1) event, and scenario events of M_w=6.5 as well as M_w=6.0 in terms of the broadband and only-stochastic simulations (Figures 9-14). Node locations and numbers with a grid spacing of 0.2° in both directions are shown in Figure 8. Some nodes, which are close to the hypocenter of the 1999 Duzce earthquake or the scenario earthquakes yield unrealistic results for both the stochastic and broadband simulations due to numerical errors at close distances.

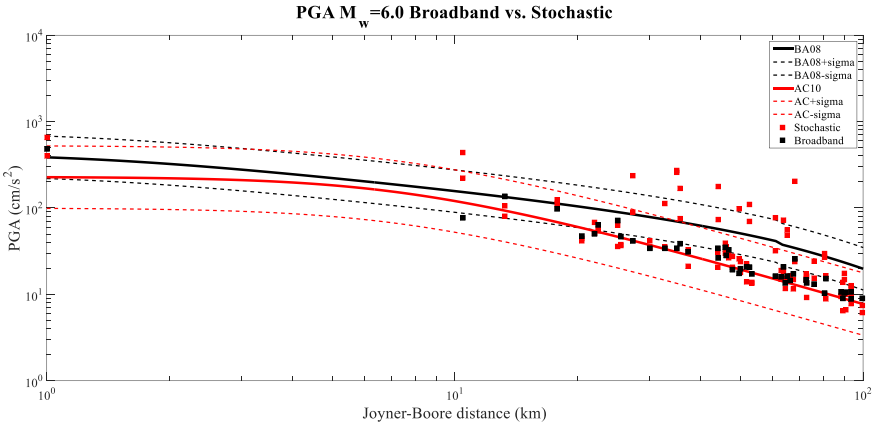

Figure 2. Comparison of the simulated PGA values from the broadband and stochastic methods with the corresponding values from the GMPE's for the scenario earthquake of M_w=6.0

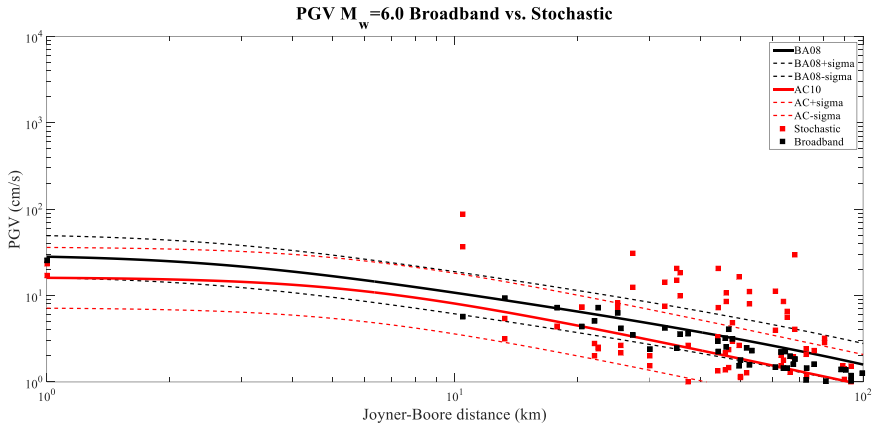

Figure 3. Comparison of the simulated PGV values from the broadband and stochastic methods against the corresponding values from the GMPE's for the scenario earthquake of M_w=6.0

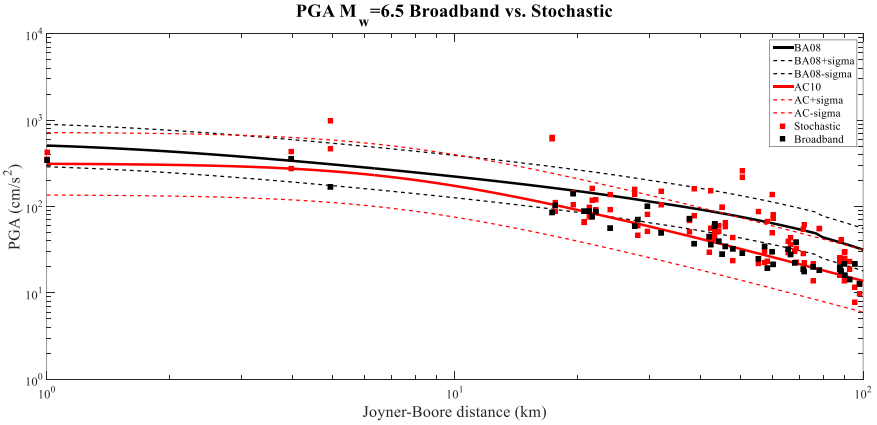

Figure 4. Comparison of the simulated PGA values from the broadband and stochastic methods against the corresponding values from the GMPE's for the scenario earthquake of M_w=6.5

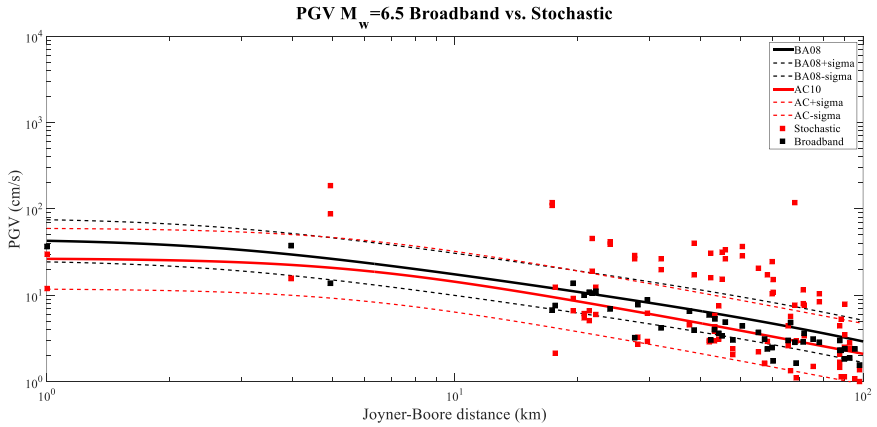

Figure 5. Comparison of the simulated PGV values from the broadband and stochastic methods against the corresponding values from the GMPE's for the scenario earthquake of M_w=6.5

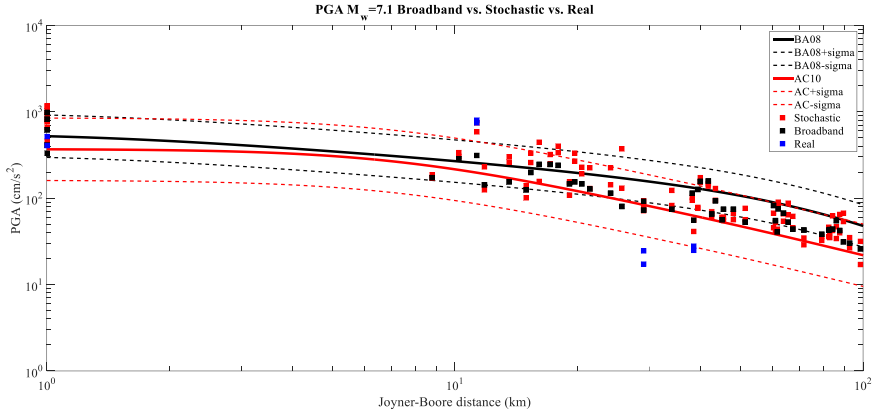

Figure 6. Comparison of the simulated PGA values from the broadband and stochastic methods against the corresponding values from the GMPE's for the scenario earthquake of M_w=7.1 along with the results for the 1999 Duzce earthquake (M_w=7.1) at DZC, BOL, GYN and SKR stations

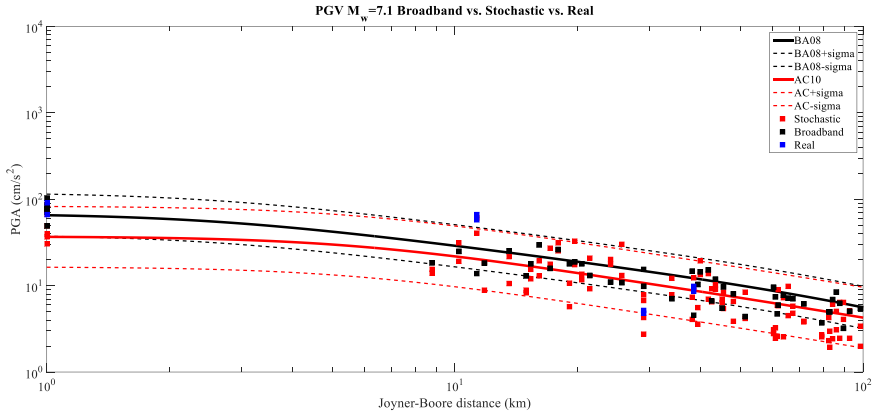

Figure 7. Comparison of the simulated PGV values from the broadband and stochastic methods against the corresponding values from the GMPE's for the scenario earthquake of M_w=7.1 along with the results for the 1999 Duzce earthquake (M_w=7.1) at DZC, BOL, GYN and SKR stations

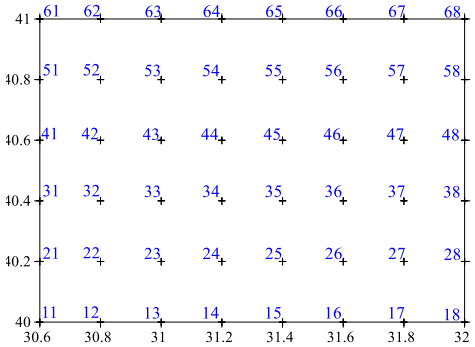

Figure 8. Selected nodes within the study area used for ground motion simulations

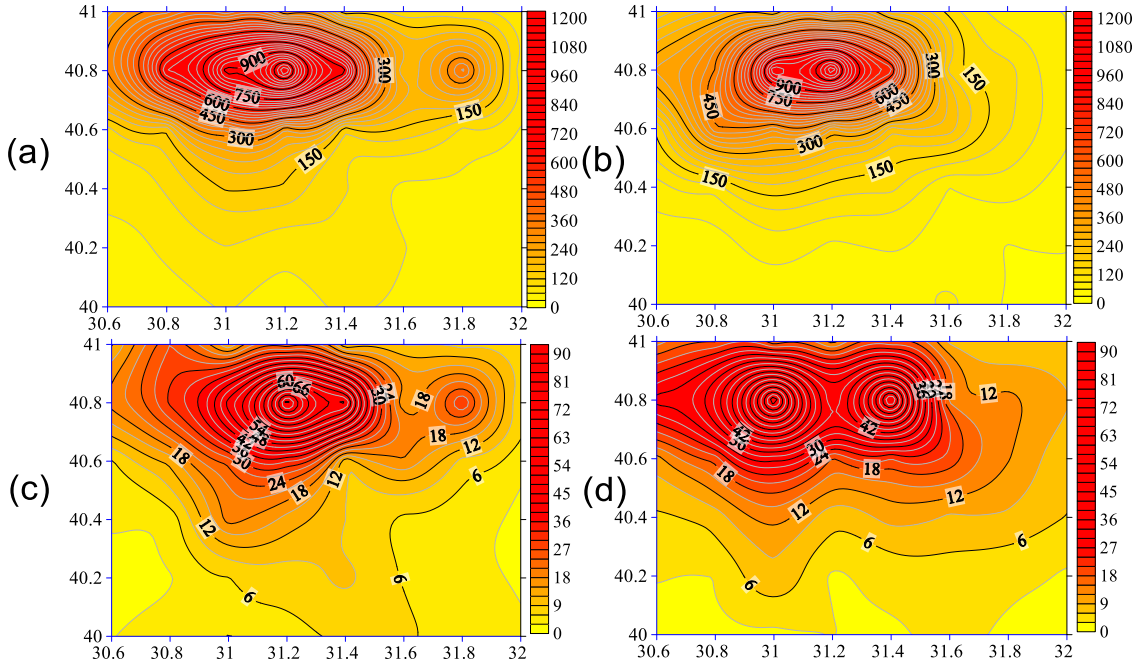

Figure 9. Spatial distribution of simulated ground motions in terms of (a) PGA (cm/s²) in EW direction, (b) PGA (cm/s²) in NS direction, (c) PGV (cm/s) in EW direction and, (d) PGV (cm/s) in NS direction for 1999 Düzce (Mw=7.1) event

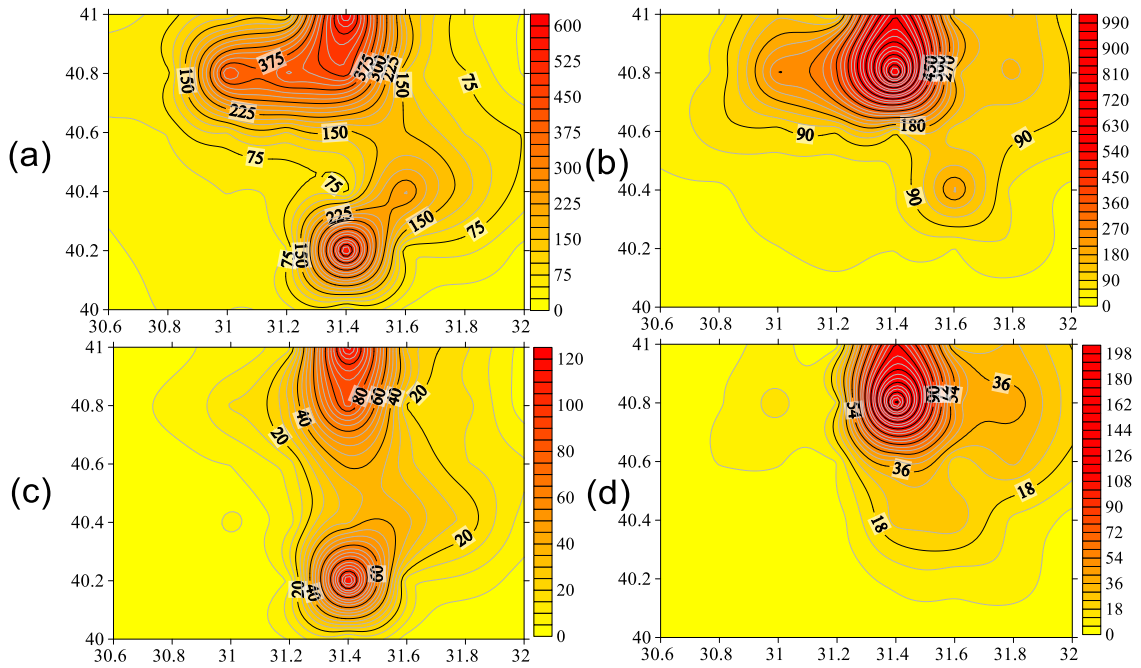

Figure 10. Spatial distribution of simulated ground motions in terms of (a) PGA (cm/s²) in EW direction, (b) PGA (cm/s²) in NS direction, (c) PGV (cm/s) in EW direction and, (d) PGV (cm/s) in NS direction for a scenario earthquake with Mw=6.5

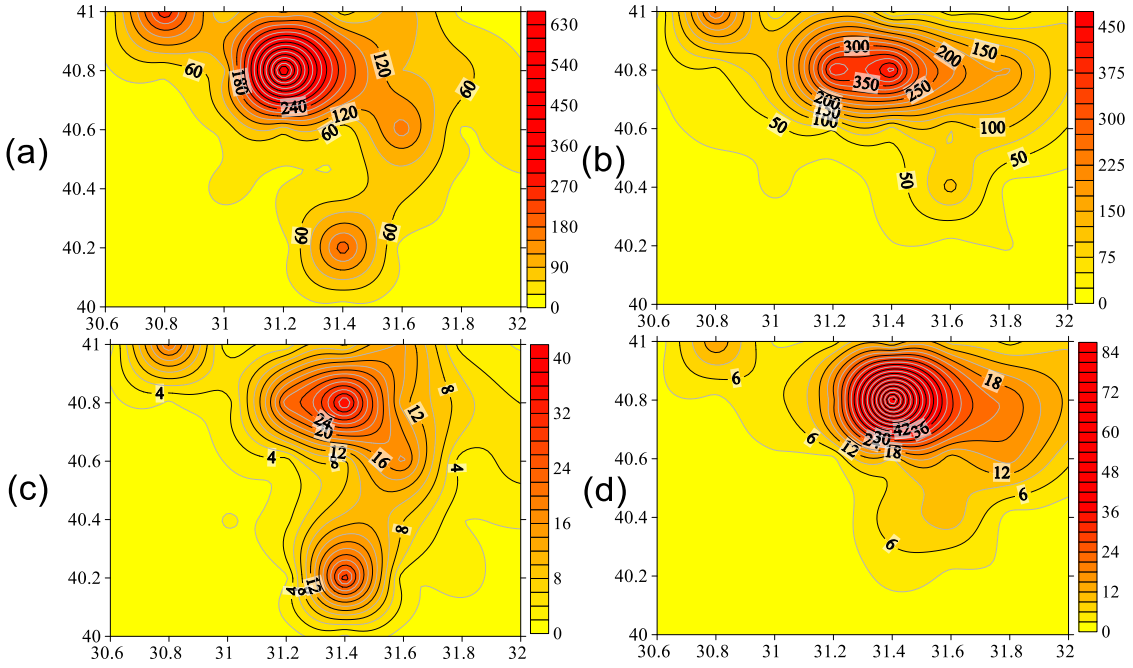

Figure 11. Spatial distribution of simulated ground motions in terms of (a) PGA (cm/s²) in EW direction, (b) PGA (cm/s²) in NS direction, (c) PGV (cm/s) in EW direction and, (d) PGV (cm/s) in NS direction for a scenario earthquake with Mw=6.0

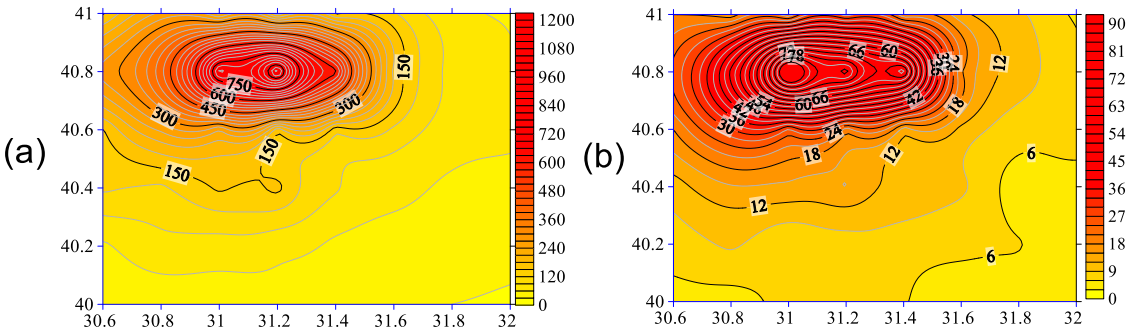

Figure 12. Spatial distribution of stochastic ground motion simulations for (a) PGA (cm/s²), (b) PGV (cm/s) for 1999 Düzce (Mw=7.1) event

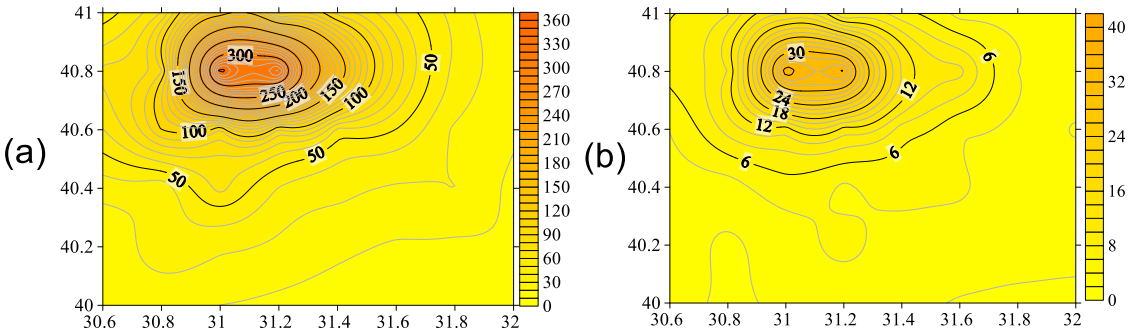

Figure 13. Spatial distribution of simulated ground motions in terms of (a) PGA (cm/s²), (b) PGV (cm/s) for a scenario earthquake with Mw=6.5

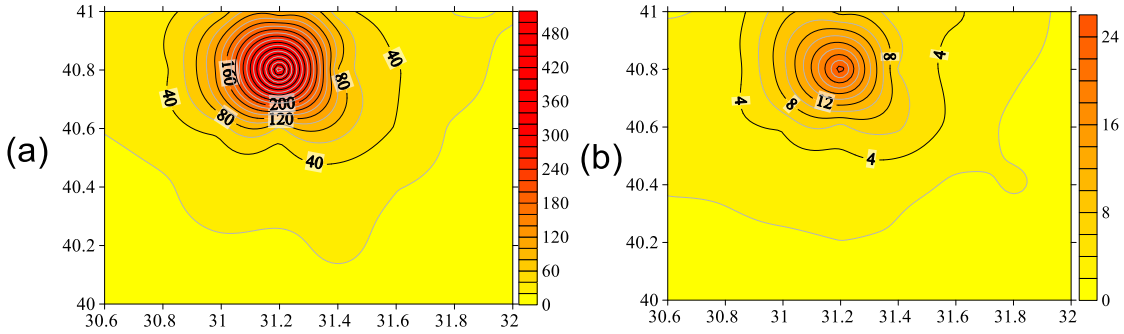

Figure 14. Spatial distribution of simulated ground motions in terms of (a) PGA (cm/s²), (b) PGV (cm/s) for a scenario earthquake with Mw=6.0

5. CONCLUSIONS

The main objective of this study is to compare the stochastic finite-fault and hybrid ground motion simulations performed for the 1999 Duzce earthquake and two scenario events with M_w=6.5 and 6.0. The comparisons are made in terms of PGA and PGV. Additionally, the results are compared against two different GMPE's: One local and one global.

The conclusions drawn from the numerical experiments performed in this study are listed as below:

- It is observed that broadband ground motion simulation method gives closer results to the real records when compared to only-stochastic ground motion simulation method.
- At near-field stations, broadband ground motion simulations may give unrealistic results due to the numerical errors at short distances arising from the deterministic ground motion simulation part.
- The results in this study suggest that broadband ground motion simulations are essential for earthquake engineering purposes, since this technique simulates the entire broadband frequency range of ground motions compared to the only stochastic one.

REFERENCES

Aki, K. (1967). Scaling law of seismic spectrum. *Journal of Geophysical Research* **72(4)**: 1217-1231.

Askan, A., Karimzadeh, S., Asten, M., Kilic ,, N., Sisman, F. N., & Erkmen, C. (2015). Assessment of seismic hazard in the Erzincan (Turkey) region: Construction of local velocity models and evaluation of potential ground motions. *Turkish Journal of Earth Sciences* **24**: 529–565.

Boore, D. M. (1983). Stochastic simulation of high-frequency ground motions based on seismological models of the radiated spectra. *Bulletin of the Seismological Society of America* **73(6)**: 1865–1894.

Boore, D. M. (2003). Simulation of ground motion using the stochastic method. *Pure and Applied Geophysics* **160**: 635–676.

Boore, D. M., and Atkinson, G. M. (2008). Ground–motion prediction equations for the average horizontal component of PGA, PGV, and 5%–damped PSA at spectral periods between 0.01 s and 10.0 s. Earthquake Spectra **24(1)**: 99–138.

Boore, D. M., & Joyner, W. (1997). Site amplifications for generic rock sites. *Bulletin of the Seismological Society of America* **87**: 327–341.

Bouchon, M. (1981). A simple method to calculate Green's functions for elastic layered media. *Bulletin of Seismological Society of America* **71(4)**: 959 - 971.

EXSIM, a FORTRAN program for simulating stochastic acceleration time histories from finite-faults with a dynamic corner frequency approach. http://www.daveboore.com/software_online.html, (last visited on December 2015).

Hartzell S. (1978). Earthquake aftershocks as Green's functions. *Geophysics. Res.* Lett. **5**: 1-4.

Hisada, Y. (1994). An efficient method for computing Green's functions for a layered half-space with sources and receivers at close depths. *Bulletin of the Seismological Society of America* **84(5)**: 1456 - 1472.

Hisada, Y. (2008). Broadband strong motion simulation in layered half-space using stochastic Green's function technique. *Journal of Seismology* **12(2)**: 265-279.

Karimzadeh, S., Askan A., Yakut A. (2017). Assessment of Simulated Ground Motions in Earthquake Engineering Practice: A Case Study for Duzce (Turkey). *Pure and Applied Geophysics* **174(9)**: 3589–3607.

Karimzadeh, S., Askan, A., Yakut A., Ameri, G. (2017). Assessment of Simulation Techniques in Nonlinear Time History Analyses of Multi-Story Frame Buildings: A Case Study. *Soil Dynamics and Earthquake Engineering* **98**: 38-53.

Motazedian, D., and Atkinson, G. M. (2005). Stochastic finite-fault modeling based on a dynamic corner frequency. *Bulletin of the Seismological Society of America* **95(3)**: 995–1010.

OpenSees 2.5.0. Computer Software, University of California, Berkeley, CA. Retrieved from http://opensees.berkeley.edu. (Last visited on May 2017)

Ozmen, E, Karimzadeh, S. and Askan, A. (2019). Broadband Ground Motion Simulation within the City of Duzce (Turkey) and Building Response Simulation. *Pure and Applied Geophysics* **24**: 1-21.

Spudich, P., ve Xu, L. (2003). Documentation of software package COMPSYN: Programs for earthquake ground motion calculations using complete 1-D Green's functions, IASPEI Handbook of Earthquake and Engineering Seismology, Academic Press, 56 pp.

Ugurhan, B., Askan, A. (2010). Stochastic strong ground motion simulation of the 12 November 1999 Düzce (Turkey) earthquake using a dynamic corner frequency approach. *Bulletin of the Seismological Society of America* **100(4)**: 1498-1512.

Umutlu, N., K. Koketsu, and C. Milkereit (2004). The rupture process during the 1999 Duzce, Turkey, earthquake from joint inversion of teleseismic and strong-motion data. *Tectonophysics* **39(1)**: 315–324.

Utkucu, M., S.S. Nalbant, J. McCloskey, S. Steacy, and O. Alptekin (2003). Slip distribution and stress changes associated with the 1999 November 12, Duzce (Turkey) earthquake (Mw = 7.1). *Geophys. J. Int.* **153(22)**: 9–241.